STABILISATION OF THE m=2 TEARING MODE WITH APPLIED HELICAL FIELDS

Tim C. Hender
Culham Laboratory, Abingdon, OX14 3DB, UK

Kurt S. Riedel
New York University, 251 Mercer Street, New York, 10012, USA

Kai Grassie
Max-Planck-Institut für Plasmaphysik, Garching, FRG

IPP 5/21 June 1988

MAX-PLANCK-INSTITUT FÜR PLASMAPHYSIK

8046 GARCHING BEI MÜNCHEN

MAX-PLANCK-INSTITUT FÜR PLASMAPHYSIK

GARCHING BEI MÜNCHEN

STABILISATION OF THE m=2 TEARING MODE WITH APPLIED HELICAL FIELDS

Tim C. Hender
Culham Laboratory, Abingdon, OX14 3DB, UK

Kurt S. Riedel
New York University, 251 Mercer Street, New York, 10012, USA

Kai Grassie
Max-Planck-Institut für Plasmaphysik, Garching, FRG

IPP 5/21 June 1988

Die nachstehende Arbeit wurde im Rahmen des Vertrages zwischen dem Max-Planck-Institut für Plasmaphysik und der Europäischen Atomgemeinschaft über die Zusammenarbeit auf dem Gebiete der Plasmaphysik durchgeführt.

STABILISATION OF THE m=2 TEARING MODE WITH APPLIED HELICAL FIELDS

T C Hender
Culham Laboratory, Abingdon, OX14 3DB, UK.

K S Riedel
New York University, 251 Mercer Street, New York, 10012 USA.

K Grassie
Max-Planck-Institut für Plasmaphysik, Garching, W Germany.

ABSTRACT

The necessary response times for feedback stabilisation of the m=2 tearing mode with externally applied m=2 helical fields are examined. Since the timescales for full penetration of the applied field are much longer than the relevant times for the feedback, the cancellation of the m=2 island by the applied field is necessarily transient. Continued penetration of the applied field leads to an island whose phase is 'flipped' relative to the initial plasma island. This flip mechanism places constraints on the helical coil current. If the feedback helical field is not exactly anti-phased relative to the plasma island, then a net torque results which also tends to flip the plasma island. This torque mechanism places constraints on the tolerable phase error and response times of the feedback helical field. For parameters consistent with JET and a phase error of 10^{o}, the necessary response time $\lesssim$ 500 μs.

1. INTRODUCTION

The major disruption limits both the achievable density and current, in the tokamak [1], and thus places constraints on beta. The disruption density limit is increased by up to a factor ∿ 2 by Neutral Beam Heating but care must be taken to step the beam and density down gradually to avoid a major disruption. The limit imposed on the current by $q_\psi \geq 2$ appears to be a fairly hard limit, although a few Tokamaks have succeeded in bettering it [2]. It is thus highly desirable to investigate means of controlling the major disruption to improve Tokamak operating parameters. Both experimentally [3] and theoretically [4,5] the m=2, n=1 tearing mode is implicated as playing a major role in the events leading up to a disruption. Thus, stabilising the m=2, n=1 tearing mode should help to prevent the major disruption. Several schemes to stabilise the m=2 tearing mode have been suggested. By locally flattening the equilibrium toroidal current near q=2, with RF current drive/heating, the driving term is removed and the tearing mode is stabilised [6]. This local flattening, however, tends to raise the current gradients elsewhere and thus destabilises other tearing modes, though tokamak profiles which are stable to all tearing modes have recently been found [7]. Another stabilisation scheme which has been suggested is to use RF to drive local currents which exactly cancel out those forming the tearing mode [8]; for a rotating mode this implies an active feedback system. The required RF power levels to stabilise the tearing mode with this scheme appear to be rather high [9]. The stabilisation method which has received the most attention experimentally, is to use helical coils, external to the plasma, to induce resonant helical fields. In experiments such as TOSCA [10] and PULSATOR [11] a steady current (DC) was applied in the helical coils, and in some cases, a stabilising effect on the oscillating m=2 mode was observed. The stabilisation presumably arises because of changes in equilibrium profiles caused by the resonant fields [10]. In other experiments on ATC [12] and T01 [13] active feedback using resonant helical fields was attempted, with some success. The active feedback in these cases involved tracking the position of the magnetic activity, and attempting to apply equal and opposite magnetic fields to cancel the mode out. Calculations assuming the ability to exactly track the mode and instantaneously apply stabilising helical fields, have shown that such a stabilisation method will work [14]. However, in practice of course, the mode position can not be exactly tracked nor can the feedback system apply the necessary fields instantaneously. In this paper, we will address the questions of the necessary accuracy in tracking the mode and the response times for the feedback system to work. In the next section, we will describe the equations used in this study and briefly discuss the codes used to solve them. In Section 3, we examine the penetration of the helical fields into the plasma and the response of the plasma to these fields. An understanding of these issues will allow us to assess the required timescales for feedback stabilisation. These issues are addressed for the specific case of the proposed JET helical coil system in Section 4. Finally, conclusions are given in Section 5.

2. EQUATIONS AND NUMERICS

In the limit of small inverse aspect ratio (ϵ) and low $\beta(\sim\epsilon^2)$ a simple set of reduced Tokamak MHD equations may be derived [15,16]. As this derivation is documented in Refs 15 and 16 we reproduce the equations here, without further comment. The magnetic field $\vec{B}$ and velocity $\vec{V}$ are represented in polar cylindrical co-ordinates as

$$\vec{B} = \vec{e}_z \times \vec{\nabla}_\perp \psi + B_o \vec{e}_z \quad \text{and} \quad \vec{V} = \vec{e}_z \times \vec{\nabla}_\perp \phi \tag{1}$$

In the limit $\epsilon \ll 1$, $\beta \sim \epsilon^2$ equations for the time evolution of ψ, ϕ may be derived from the resistive MHD equations.

$$\frac{\partial \psi}{\partial t} = \left(\frac{\partial \psi}{\partial r}\frac{1}{r}\frac{\partial}{\partial \theta} - \frac{1}{r}\frac{\partial \psi}{\partial \theta}\frac{\partial}{\partial r}\right)\phi + \frac{\eta}{S}\nabla_\perp^2 \psi + \frac{\partial \phi}{\partial z} \tag{2}$$

and

$$\frac{\partial \nabla_\perp^2 \phi}{\partial t} + \left(\frac{\partial \phi}{\partial r}\frac{1}{r}\frac{\partial}{\partial \theta} - \frac{1}{r}\frac{\partial \phi}{\partial \theta}\frac{\partial}{\partial r}\right)\nabla_\perp^2 \phi =$$

$$\left(\frac{\partial \psi}{\partial r}\frac{1}{r}\frac{\partial}{\partial \theta} - \frac{1}{r}\frac{\partial \psi}{\partial \theta}\frac{\partial}{\partial r}\right)\nabla_\perp^2 \psi + \frac{\partial \nabla_\perp^2 \psi}{\partial z} \tag{3}$$

where

$$\nabla_\perp^2 = \frac{1}{r}\frac{\partial}{\partial r} r \frac{\partial}{\partial r} + \frac{1}{r^2}\frac{\partial^2}{\partial \theta^2} \tag{4}$$

In these equations, all lengths are normalised to the minor radius 'a'; the poloidal flux ψ is normalised to by $B_o a^2$, where B_o is the toroidal field strength; time is normalised to the poloidal Alfven transit time $\tau_{Hp} = a\sqrt{\rho_o}/(\epsilon B_o)$ where ρ_o is the peak density; and $S = \tau_R/\tau_{Hp}$ is the so-called 'Magnetic Reynolds Number' with $\tau_R = a^2/\eta_o$ being the resistive diffusion time, where η_o is the peak resistivity.

Near the origin, the boundary conditions for Eqs (2) and (3) are given by regularity

$$\phi, \psi \ \alpha \ r^{|m|} \tag{5}$$

where m is the poloidal mode number. At the edge (r=1), we consider the idealised situation of a plasma in contact with the helical coils which are in turn surrounded by an infinite vacuum region. In practice, the helical coils are discrete and have a broad toroidal and poloidal Fourier spectrum. Here, however, we are only interested in the effect of the m=2, n=1, fields and thus only consider that Fourier component of the coil current. Therefore, at the plasma vacuum interface, we consider a sheet current

$$I_c \operatorname{Cos}(2\theta + \xi) \tag{6}$$

(the current flowing in the plus or minus direction of the poloidal cross-section is $2I_c$).

Here, and throughout this paper, we assume without loss of generality that the coil only has a Cosine component. At the edge the boundary condition on ψ_c Cos(2θ + ξ) is given by

$$r \frac{\partial\psi_c}{\partial r} = -|m|\ \psi_c + I_c \tag{7a}$$

and for all remaining components of ψ the edge boundary condition is

$$\frac{\partial\psi}{\partial r} = \frac{-|m|}{r}\ \psi \tag{7b}$$

The boundary condition on the velocity stream function ϕ is less well determined. We use the condition that no radial flow may occur across the coil surface (r=1) which gives ϕ(r=1) = 0. It should be noted that this boundary condition leads to a resistive layer at r=1 [17]. We have, however, tried alternate boundary conditions on ϕ and find that the results are not sensitive to this boundary condition.

Numerically, we advance Eqs (2) and (3) using a Fourier representation in θ and ξ, and finite differences in the radial direction. We have used two distinct codes to solve these equations, one of which uses an explicit time centred scheme with the $\nabla^2_\perp$ terms included implicitly [18], and the other which includes all linear terms implicitly [19]. Detailed and favourable comparisons between these two codes serve as a valuable validation of the numerics.

3. RESULTS

We will first study how the helical field penetrates into the plasma and then examine the interaction of this field with an existing m=2 tearing mode island. We will identify two distinct processes associated with this interaction. First, because the penetration of the applied helical field occurs on a fractional resistive timescale, a quasi-steady state is only reached after a time which is far longer than relevant times for the feedback (eg plasma rotation time). Thus, exact cancellation of the intrinsic plasma island, by the applied helical field, is necessarily transient. Thereafter, a magnetic island grows in phase with the helical coil (and opposite to the intrinsic plasma island). This island grows both due to the continued penetration of the helical field, and also due to the intrinsic tearing instability in the new phase. This ability of the tearing instability to 'flip' is discussed by Monticello et al [20]. A second distinct process occurs if, as must occur in practice, the plasma island and applied helical field are not exactly anti-phased. In this case, a net torque arises between the plasma island and the helical coil. The effect of which is also to flip the plasma island and align it with the phase of the helical coil island, thus defeating the feedback system. To distinguish these two flip mechanisms, we adopt the terminology of calling the first the 'flip' and the second the 'torque mechanism'.

3.1 Penetration of Helical Field

We start by studying how the m=2, n=1 applied helical field penetrates into the plasma. Many of the phases in this process are discussed by Hahm and Kulsrud [21], and the additional effect of viscosity is considered by Park et al [22].

Insight into the field penetration process may be gained by deriving a simple dispersion relation from Eqs (2) and (3). Linearising, the ideal ($\eta=0$) equations, introducing radial, k_r and parallel $k_{||}(=\vec{K}.\vec{B}_{eq})$ wavelengths and a growth rate ω we find in leading order that

$$(\omega^2 - k_{||}{}^2)k^2{}_r - \frac{m}{r} k_{||}J_z' - (k_{||}{}^2)' K_r = 0 \qquad (8)$$

where primes denote differentiation with respect to r. In the limit of no shear (J_z = constant), we recover the Alfven wave dispersion relation. This gives propagation parallel to $\vec{B}_{eq}$ but no radial penetration of the magnetic field. Introducing the shear we obtain radial propagation both from the J_z term and because $k_{||}$ =

$k_{||}(r)$. Resistive diffusion can also play a role in the radial penetration of the magnetic field. This is particularly true near the edge, where the applied helical fields cause large current gradients. Away from the edge, however $k_r \sim 1$ and the inward propagation is due to the shear (and independent of resistivity). As q=2 is approached, $k_{||} \to 0$ and a sheet current is set up near q=2. Physically, this sheet current is set up to resist tearing of the field and formation of an m=2 island on an Alfvenic timescale. On a fractional resistive timescale, the field can tear and allow island formation. Several possible regimes relating to island formation are studied in Ref 21. These results are borne out by the numerical solutions. To study the penetration phase, it is convenient to study equilibria which are intrinsically stable to the m=2, n=1 tearing mode; this avoids any confusion arising between the penetrating fields and a growing tearing mode. Here we study the profile $q = 0.7(1 + 2.75 r^2)$ which has $\Delta'_{2,1} = -0.71$. Initially on application of the helical coil current we find a sharp spike in the perturbed m = 2, n = 1 toroidal current at the edge (r = 1). A similar spike in the current was observed by Park et al [22]. This current spike diffuses resistively into the plasma. At the singular surface, however, the evolution of current is relatively independent of resistivity.

The various regimes discussed in Ref 21 give different scalings for the evolution of the m=2, n=1 current at the singular surface ($\tilde{J}_Z(r_s)$) and for the formation the magnetic island. In the linear regime after the Alfvenic penetration of the sheet current a normal tearing mode type scaling gives the island width, $W \alpha t^{5/8} (\eta/S)^{3/8} \surd I_C$. While in the non linear regime a Rutherford like scaling occurs, $W \alpha (I_C \eta t/S)^{1/3}$. The associated evolution of $\tilde{J}_Z(r_s)$ is given by the identity

$$\frac{dW^2}{dt} = \frac{16q^2}{rq'} \frac{\eta}{S} \tilde{J}_Z(r_s) \qquad (9)$$

Hence in the linear tearing regime $\tilde{J}_Z(r_s) \alpha (I_C{}^2 WS/\eta)^{2/5}$ and in the non linear regime $\tilde{J}_Z(r_s) \alpha I_C/W$ (and independent of S). After the initial penetration of the fields the linear tearing regime is observed numerically. This is demonstrated by plotting $W(S/\eta)^{3/8} I_C^{-1/2}$ versus $t^{5/8}$ in Fig 1(a). The applied helical current is $I_C = 10^{-7}$ and results are shown for $S=10^5$ and 10^6; it can be seen that the linear tearing scaling is obeyed well. We have also tested the scaling $W \alpha \surd I_C$ in this regime and find it is obeyed to excellent accuracy. For larger applied helical currents after an initial phase the non linear Rutherford like scaling is obeyed to reasonable accuracy; this is demonstrated in Fig 1(b) by plotting $W(S/I_C)^{1/3}$ versus $t^{1/3}$ for various values of S and I_C. Closer examination of scalings in this case however, show that numerically $W \alpha S^{-0.28}$ (as opposed to the analytic prediction of $W \alpha S^{-0.33}$).

After a long time, the radial magnetic field will limit to the $\Delta'_{2,1} = 0$ solution of the marginal stability equation:-

$$K_{\|} \nabla_{\perp}^2 \psi - \frac{m}{r} \psi \frac{dJ_{zeq}}{dr} = 0 \qquad (10)$$

Thus the steady state radial magnetic field is independent of resistivity. However, the evolution of field and time to reach steady state is strongly dependent on the resistivity [cf Eq(9)]. Figure 2 shows the $\psi_{2,1}$ evolution at various times for $S = 10^6$ and $q = 0.7 (1 + 2.75r^2)$. It can be seen that the time to reach steady state $\sim 0.05 \tau_R$. From Eq(9) we expect the time for the radial field to penetrate to scale as S^{-1} in the non linear regime. Thus for JET where $\tau_R \sim 10$ sec, we see that the applied field will not fully penetrate on the timescales of the feedback ($\sim$ 0.1 to 1 ms). Thus, as discussed in the introduction to this section, the cancellation of intrinsic plasma island by the applied helical field will be transient.

3.2 The Flip Mechanism

In order to find a description of the variation of island width with time we choose the following representation of magnetic flux:

$$\psi_{2,1} = (\alpha(t)\psi_t + I_C\psi_h)e^{i(2\theta + \xi)} \qquad (11)$$

where ψ_t, ψ_h are solutions of the marginal force balance, Eq (10), with $\psi_t(r_s) = 1$, $\psi_h(r_s) = 0$, and at the edge ($r = 1$) ψ_t satisfies the tearing mode boundary condition [Eq 7(b)] and ψ_h satisfies the helical coil boundary condition [Eq 7(a), with $I_C = 1$]. The flux reconnecting on the island separatrix is determined by the current at the X-point

$$\frac{d\alpha}{dt} = \frac{\eta}{S} J_z(r_x) \qquad (12)$$

The various scalings for reconnection are equivalent to scalings for $J_z(r_x)$ given the total current. For a forced reconnection, such as occurs when the helical coils are turned on, Sweet-Parker reconnection [$J_z(r_x) \; \alpha (\eta/S)^{-1/2}$] can occur. For strongly forced reconnection other scalings can occur [24]. For non-driven reconnection the current inside the island is to lowest order constant and independent of resistivity. In this case Rutherford reconnection occurs and the island width (W) evolution is given by [25]

$$\frac{dW}{dt} = 1.66\, \Delta_t' \frac{\eta}{S} \tag{13}$$

It should be noted that the Rutherford scaling of the tearing mode is reproduced by our numerical simulations to excellent accuracy.

The island width variation in the general case including forced reconnection due to the helical coil is essentially a combination of Eqs (9) and (13)

$$\frac{dW}{dt} = 1.66\, \Delta_t' \frac{\eta}{S} + \frac{8q^2}{r_s q'} \frac{\eta}{WS} J_h(r_s) \tag{14}$$

In the non linear regime the current due to the helical coil, $J_h \alpha I_c (S/\eta)^{\delta}/W$; analytically δ=0 but as noted above the numerical results indicate δ=0.14. Substituting for J_h into Eq(14) we have

$$\frac{dW}{dt} = \frac{a\eta}{S} - b\, \frac{(\eta/S)^{1-\delta} I_c}{W^2} \tag{15}$$

with $a \equiv 1.66\, \Delta_t'$ and $b \equiv \frac{8q^2}{r_s q'}\, c$.

This equation can easily be integrated, yielding the implicit time dependence of the island width

$$t = \frac{S}{\eta a} [W(t) - W_o + \sqrt{\lambda}\, \tanh^{-1} (\frac{\sqrt{\lambda}(W_o - W(t))}{\lambda - W_o W(t)})] \tag{16}$$

where W_o = W(t = 0), and $\lambda = bI_c(\eta/S)^{-\delta}/a$.

In Fig 3 we plot the island size versus time for several different resistivities and a helical coil current of $I_c = 2 \times 10^{-3}$. The equilibrium in this case, $q = 1.1\ (1 + 232r^8)^{1/4}$, is tearing mode unstable and the calculation is initiated with a 4.2%, m = 2 island at t = 0. The other parameters are $\eta \alpha 1/J_z$, with the phase of the helical coil island exactly opposite (180° in ξ) to the initial plasma island. Results of the full numerical treatment are represented in Fig 3 by the solid lines, whereas dashed curves correspond to the analytical solution, Eq(16). The required constants (a, b) in Eq(16) are obtained from solving with $I_c = 0$ (see Fig 4) which gives a = 2.36 (for this equilibrium) and b = 49.5, is obtained by matching to the time to drive W to zero at S = 10^6 (see Fig 3). There is reasonable agreement between numerical and analytical results in Fig 3. Note that slight deviations for the S = 10^5 case are probably due to effects of the current penetration phase which are not taken into account in the analytic analysis. In Fig 4 an equivalent comparison of Eq(16) with the numerical results is made for various helical coil currents with $S=10^6$. Again there is reasonable agreement between the analytic and numerical results; the worse agreement at the lower current ($I_c=2.5 \times 10^{-3}$) is probably due to this case having a longer linear phase. From Eq(16), and from Figs 3 and 4, we see that after the island width has reached zero, it then grows again, but with its phase 'flipped' to align itself to the phase determined by the helical coil. For the feedback system to work, this flip time (τ_f) must be longer than the feedback system response time (τ_o); this places an upper limit on I_c. Alternatively a lower limit on I_c is placed by the requirement that the island width decreases in time (dW/dt<0). Thus the role of the phase flip is not to determine τ_o but is to determine the permissible range for I_c. Estimates of required I_c will be given in Section 4.

3.3 Torque Mechanism

In the previous section, we assumed that the helical coil field was exactly anti-phased to the intrinsic plasma island. Of course, in practice there will be a relative phase error between these two fields and as we shall show, this leads to a net-torque which causes the island to rotate. This torque mechanism is discussed in Ref 26. Ignoring the convective derivative term in Eq (3), integrating twice by parts over r, and averaging over θ, z gives

$$\frac{d}{dt}\int_0^1 r^2 V_{\theta o}\, dr = \frac{m}{2}\left[\frac{\partial\psi_c}{\partial r}\psi_s - \frac{\partial\psi_s}{\partial r}\psi_c\right]_0^1 \qquad (17)$$

where the subscripts 'c' and 's' denote Cosine and Sine components respectively, $V_{\theta o}$ is the m=0, n=0 poloidal flow (= $d\phi_{o,o}/dr$) and we have retained only the m=2, ψ components. Using the boundary conditions Eq (7) we find that

$$\frac{d}{dt}\left[\int_0^1 r^2 V_{\theta o}\, dr\right] = \frac{m}{2} I_c \psi_s|_{r=1} \qquad (18)$$

where we are using the assumption that the helical coil only has a Cosine component. Hence the magnitude of ψ_s determines the phase error between the Cosine helical coil field and the magnetic island. We will denote the phase error as θ_o in the poloidal plane. From Eq(18) we then find that

$$\frac{d}{dt}\left[\int_0^1 r^2 V_{\theta o}\, dr\right] \;\alpha\; I_C W^2 \sin 2\theta_o \tag{19}$$

This equilibrium poloidal flow ($V_{\theta o}$) results in the plasma island rotating to align itself with the phase determined by the helical coils. The timescale of this torque rotation places an upper limit on the response time of the feedback system (τ_o).

We may calculate this spin time from the helical coil (ψ_t) and tearing mode (ψ_t) basis functions introduced in the previous section. Neglecting parallel viscosity we find that the island can slip over the magnetic surfaces outside the island. To calculate the acceleration of the island due to the torque we integrate the m=n=0 poloidal component of the equation motion across the island.

$$\rho r_s W \frac{dV_{\theta o}}{dt} = \frac{\rho r_s^2 W}{m}\frac{d^2\theta_o}{dt^2} = \frac{m}{2r_s}\int_{r_s-W/2}^{r_s+W/2} r\,\mathrm{Im}(\psi(r_s) J_z(r))\, dr \tag{20}$$

We note that this integral may be represented in terms of the basis function as

$$\frac{1}{r}\int_{r_s-W/2}^{r_s+W/2} rJ_z dr = \left[\frac{d\psi}{dr}\right]_{r_s-W/2}^{r_s+W/2} = \alpha(t)\,\Delta_t'(W) + \Lambda I_C \tag{21}$$

where Λ is the discontinuity in $d\psi_h/dr$ at r_s.

Thus

$$\frac{d^2\theta_o}{dt^2} = \frac{1}{32}\frac{m^2 I_C q' W\Lambda}{\rho r_s q^2}\sin 2\theta_o = C_1 I_C W \sin 2\theta_o \tag{22}$$

We may solve this equation in the limit that the initial angle, θ_I<<1 and that $\sqrt{(2C_1 I_C W)}t$<<1 to find

$$\frac{d\theta_o}{dt} = mV_{\theta_o} = 2\,\theta_I C_1 I_C W t \tag{23a}$$

and

$$\theta_o = \theta_I(1 + C_1 I_c W t^2) \qquad (23b)$$

These results are again borne out by the numerical simulations. Figure 5 shows that the relation Eq (18) is well obeyed by code. The equilibrium in this case is again $q = 1.1(1 + 232\, r^8)^{1/4}$ with $S=10^6$, $\eta=1/J_z$, $I_c = 10^{-5}$, $\theta_o = 45°$ and an initial island, $W_I = 3\%$. In fact, apart from ignoring the convective derivative Eq (18) is exact and confirmation of it with the code provides a useful check on the numerics. Figure 6 shows the various scalings predicted by Eq 23(b) are reproduced by the code; Figure 6(a), (b) and (c) showing the I_c, θ_I and W scalings respectively. The curves do not show the linear time dependence predicted by Eq 23(b); this appears to be because W changes in time an effect not considered in deriving 23(b).

The 'flip mechanism' discussed in the previous section also produces an apparent variation of the island phase. Hence, to determine the contribution of the torque mechanism to the change in island phase, we calculate the change in phase with the torque mechanism artificially suppressed (ie, $V_{\theta_o} \equiv 0$) and subtract the result from the equivalent case with the torque mechanism enabled. In this manner, we can calculate the change in phase ($\delta\theta$) caused by torque mechanism (alternatively as in Fig 6 we can use V_{θ_o} as a direct measure of the strength of the torque mechanism). Figure 7 shows that the change in phase ($\delta\theta$) is weakly dependent on S, by plotting $\delta\theta$ time for $S = 10^6$ and 3×10^6, the equilibrium being the same as that for Figs (5) and (6).

4. PARAMETERS FOR JET FEEDBACK

We are now in a position to examine the constraints on a feedback system imposed by the flip and torque mechanisms described in the last section.

The equilibrium dependent constant C_1 in Eq(22) may be estimated for the cases considered in Figs 5 and 6, to be ~ 6. If we consider the coil island to have a poloidal phase of 90° and let θ_I be the initial phase of the plasma island, then the time (τ_{spin}) for the torque mechanism to rotate the island from θ_I to 90° is

$$\tau_{spin} = \int_{\theta_I}^{\pi/2} \frac{d\theta}{(C_1 I_c W)^{1/2}\,(\cos 2\theta_I - \cos 2\theta)^{1/2}} = \frac{I(\theta_I)}{(C_1 I_c W)^{1/2}} \qquad (24)$$

Evaluating $I(\theta_I)$, numerically for $\theta_I = 5°$, $10°$ and $20°$ gives $I(\theta_I) = 2.7$, 2.22 and 1.76, respectively. To evaluate this time (τ_{spin}) we must determine the necessary helical coil current I_c. In Section 3.2, it was shown that the role of the helical coil current is to control the timescale for the plasma island to be reduced in size by the applied helical field. Unfortunately, it was also shown that continued penetration of the applied field leads to a flip instability. Thus, for the feedback to work, we must apply a helical field that is large enough for the field to penetrate and the island to be reduced in size but small enough that the flip mechanism does not exceed the response time of the feedback system.

The requirement that the island width be reduced in size by the feedback current in the helical coil is given by Eq 15,

$$\frac{b(\eta/S)^{\delta} I_c}{W^2} > a \qquad (25)$$

For JET like parameters ($S=5x10^7$, $W=3\%$) this gives $I_c > 5x10^{-4}$ (or current in helical coil >0.05% of the plasma current); where the parameters a, b are taken to be those relating in Figs 3 and 4.
For this value ($I_c = 5 \times 10^{-4}$), the spin time [Eq (24)] assuming a phase error of $\theta_I = 10^0$ is 240 τ_{Hp} which $\sim$ 0.05 ms. These values may be scaled to other assumed parameters by noting that $I_c \alpha W^2$ from Eq (25) and $\tau_{spin} \sim (WI_c \sin 2\theta_I)^{-½}$ from Eq 23(b). This spin time (0.05 ms) may seem rather rapid but it must be remembered that the simple MHD model used includes no viscosity effects which would tend to couple the flow ($V_{\theta o}$) in the vicinity of the island to the rest of the plasma. If the whole plasma rotates poloidally with the island then the spin time becomes 0.5 ms. Further if poloidal rotation is inhibited by neo-classical effects then the toroidal torques, which are ϵ smaller, will lead to $1/\sqrt{\epsilon}$ longer spin times. In fact comparing the acceleration (and deceleration) of rotating m=2 instabilities with applied helical fields on TOSCA [10] does indicate that the observed effects are weaker than those which would be expected from poloidal torque and are more consistent with the strength of the toroidal torque.

5. SUMMARY

The necessary timescales and currents for a helical field system to feedback and stabilise the m=2 tearing mode, have been studied. Analytic and numerical solution of the reduced tokamak equations have been used to analyse two effects which play a role in determining the feedback system parameters. Firstly, since the time for full penetration of the applied helical field ($\sim 0.05\ \tau_R$) is far longer than relevant timescales ($\lesssim 1$ ms), the cancellation of the plasma island by the applied field is necessarily transient. Continued penetration of the applied field then leads to a rapidly growing island in phase with the applied field. These considerations mean that the helical coil current must be large enough to cause the m=2 island size to be reduced in time but not so large that the mode flips in a time less than the response time of the feedback system. The second mechanism which dictates the timescale for the feedback, occurs because the feedback field is inevitably not exactly anti-phased with the plasma island. The result is a net torque which causes the plasma island to align itself with the island of the applied field, thus defeating the feedback system. Estimates for JET with a 3% plasma island and 10^{o}phase error show a required response time from the feedback ~ 0.05 ms (0.5 ms if the whole plasma rotates), and a current in the coils of $\gtrsim 0.05\%$ of the plasma current. It must be remembered, however, that the 'coils' are idealised and produce a pure m=2 $\vec{B}$ field. For realistic discrete coils (with a broad Fourier spectrum), the required currents will be larger.

ACKNOWLEDGEMENTS

The authors wish to thank Dr K Lackner for drawing their attention to the possibility of feedback destabilisation on an Alfvenic timescale. We should also like to thank Dr D Biskamp for useful discussions, and Drs Biskamp and Welter for providing us with a copy of their reduced MHD code. This work was financed in part by a task agreement between Culham Laboratory and the JET Joint Undertaking. Also, finances for travel were provided by a Euratom Mobility Contract. Funding for KSR was provided by the US DoE under contract #De-FG02-86ER53223 as part of the US-ASDEX exchange.

References

[1] J Hugill, Proc 2nd Int Symp on Heating in Toroidal Plasmas, Como 1980.

[2] R Birch et al, Proc 9th Eur Conf on Controlled Fusion and Plasma Physics, Oxford, 1980.

[3] S Von Goeler, W Stodiek, N Sauthoff, Nucl Fusion 18 (1978) 1445.

[4] B A Carreras et al, Phys Fl 23, (1980), 1811.

[5] J A Wesson, A Sykes, M F Turner, 10th IAEA Conf on Plasma Physics and controlled Fusion, London 2 (1985) 28.

[6] T C Hender, D C Robinson, J A Snipes, 11th IAEA Conf on Plasma Physics and Controlled Fusion, Kyoto 1 (1986) 291.

[7] C Z Cheg, H P Furth, A H Boozer, Plasma Physics and Controlled Fusion 29 (1987) 351.

[8] D W Ignat, P H Rutherford, H Hsuan, Princeton Lab Report PPL-2278.

[9] P H Rutherford, Princeton Lab Report PPL-2277.

[10] J J Ellis et al, 10th IAEA Int Conf on Controlled Fusion and Plasma Physics, London 1 (1984) 363.

[11] F Karger et al, 5th IAEA Conf on Controlled Fusion and Plasma Physics, Tokyo 1 (1974) 207.

[12] K Bol et al, 5th IAEA Conf on Controlled Fusion and Plasma Physics, Tokyo 1 (1974) 83.

[13] V V Arsenin et al, 7th IAEA Conf on Controlled Fusion and Plasma Physics, Innsbruck 1 (1978) 233.

[14] J A Holmes, B A Carreras, H R Hicks, S J Lynch, B V Waddell, Nucl Fus 19 (1979) 1333.

[15] H R Strauss, Phys Fluids 20 (1977) 1354.

[16] B V Waddell, B A Carreras, H R Hicks, J A Holmes, Phys Fluids 22 (1979) 897.

[17] C G Gimblett, Proc of Physics of Mirror, Reversed Field Pinches and Compact Torri, Varenna 1987.

[18] D Biskamp, H Welter, Proc 9th IAEA Conf on Cont Fusion and Plasma Physics, Baltimore 3 (1982) 373.

[19] T C Hender, C G Gimblett, D C Robinson, 13th European Conf on Controlled Fusion and plasma Heating, Schliersee 1 (1985) 61.

[20] D A Monticello, R B White, M N Rosenbluth, 7th IAEA Conf on Controlled Fusion and Plasma Physics, Innsbruck 1 (1978) 605.

[21] T S Hahm, R M Kulsrud, Phys Fluids 28 (1985) 2415.

[22] W Park, D A Monticello, R B White, Phys Fluids 27 (1984) 137.

[23] E N Parker, J Geophys Res 62 (1957) 509.

[24] D Biskamp, Proc of Magnetic Reconnection and Turbulence Int Workshop, Cargese 1 (1985) 19.

[25] P H Rutherford, Phys Fluids 16 (1973) 1903.

[26] E Lazzaro, F Nave, JET Report JET-P(87)54.

Figure Captions

Fig 1 Comparison of expected scalings for penetration of fields in (a) the linear phase and (b) the non linear Rutherford regime. The broken line in (b) is that predicted by the scaling law.

Fig 2 Penetration of magnetic field from (2,1) helical coil for tearing mode stable equilibria [$q = 0.7\ (1 + 2.75\ r^2)$].

Fig 3 Time evolution of 4.2% (2,1) magnetic island when a helical current $I_c = 4 \times 10^{-3}$ is applied. Results are shown for several S values, the solid curves are the numerical results and the broken curves are from Eq (16).

Fig 4 (2,1) Magnetic island width evolution for various I_c, all other parameters as Fig 3.

Fig 5 Comparison of $\frac{d}{dt}\ [\int_0^1 r^2 v_{\theta_0}\ dr]$ computed directly numerically and evaluated from Eq (18).

Fig 6 Scaling for Maximum of $V_{\theta o}$ (at $\sim r_s$) with, (a) I_c for θ_I=0.1, W = 3.6%, (b) θ_I for W_I=4.24%, I_c=10^{-4} and (c) W_I for I_c=10^{-4}, θ_I=0.1, in all cases S=10^6. The broken curve in each case is the scaling law prediction for the upper curve from the lower curve values.

Fig 7 Variation of $\delta\theta$ with time for $I_c = 5 \times 10^{-5}$, $\theta_o = 45°$, and S = 10^6, 3×10^6.

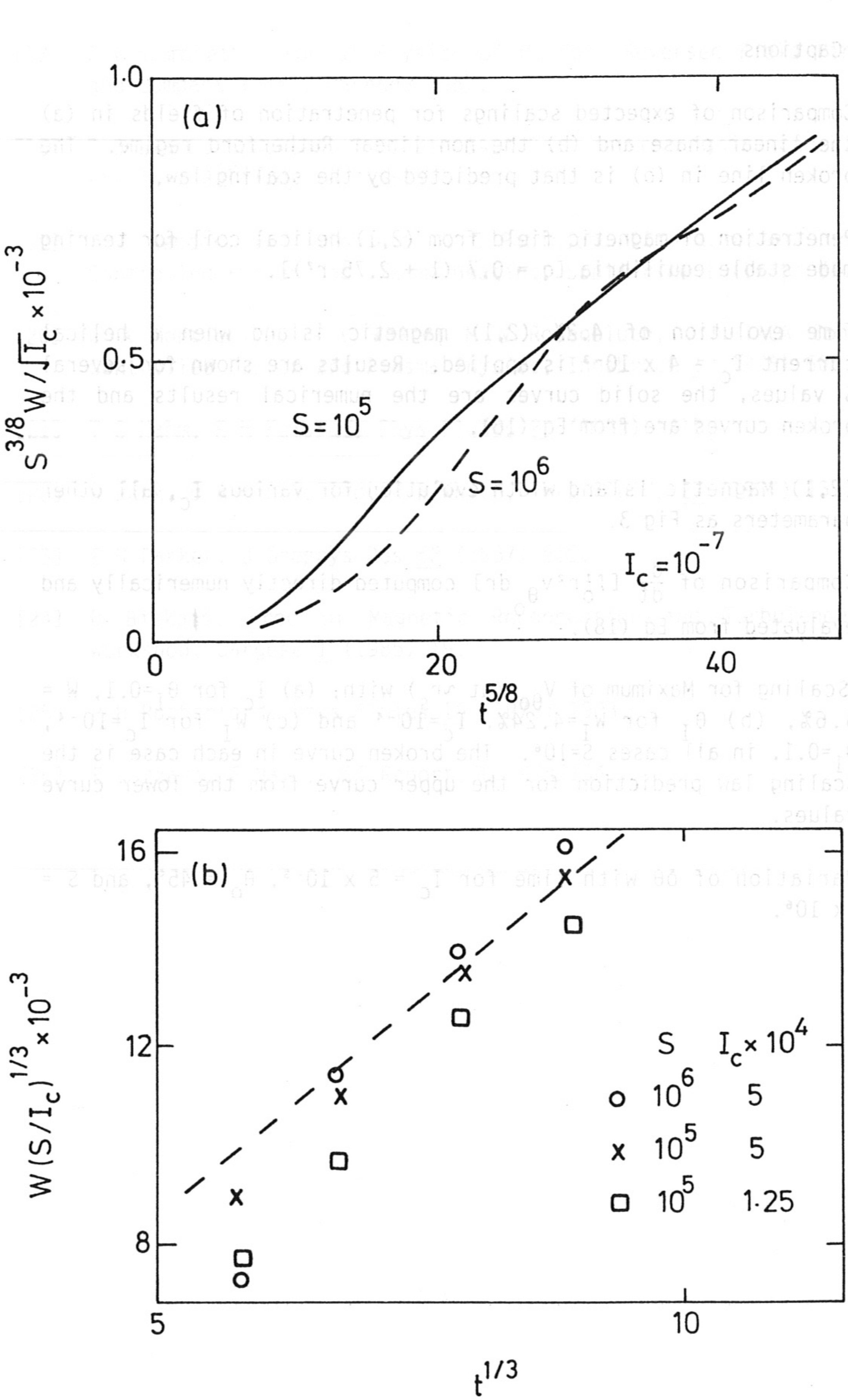

(a)
1.0
0.5
0
$S^{3/8}W/\sqrt{I_c} \times 10^{-3}$
$S=10^5$
$S=10^6$
$I_c=10^{-7}$
0
20
40
$t^{5/8}$
(b)
16
12
8
$W(S/I_c)^{1/3} \times 10^{-3}$
S
$I_c \times 10^4$
o 10^6 5
x 10^5 5
□ 10^5 1·25
5
10
$t^{1/3}$

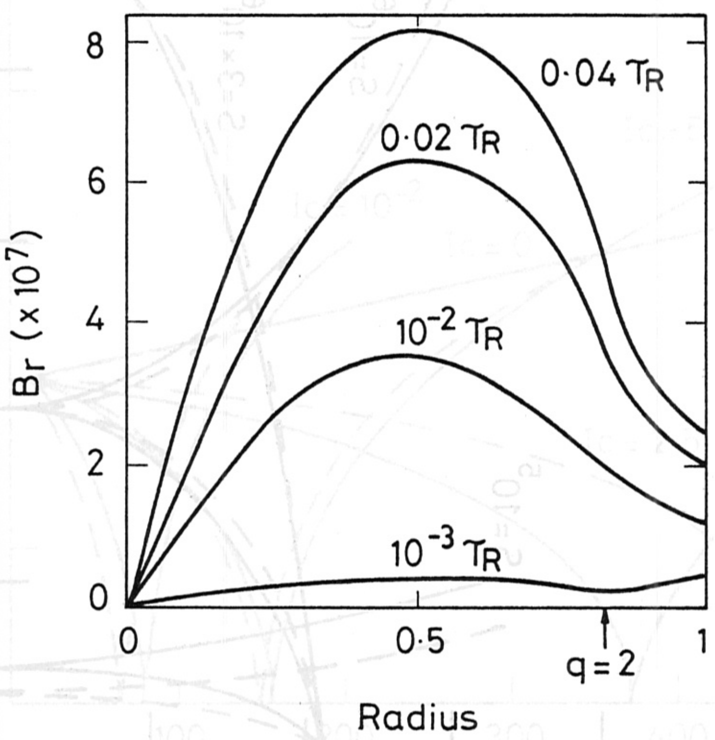

B_r (x 10^7)
8
6
4
2
0
0
0·5
1
Radius
q = 2
0·04 τ_R
0·02 τ_R
10^{-2} τ_R
10^{-3} τ_R

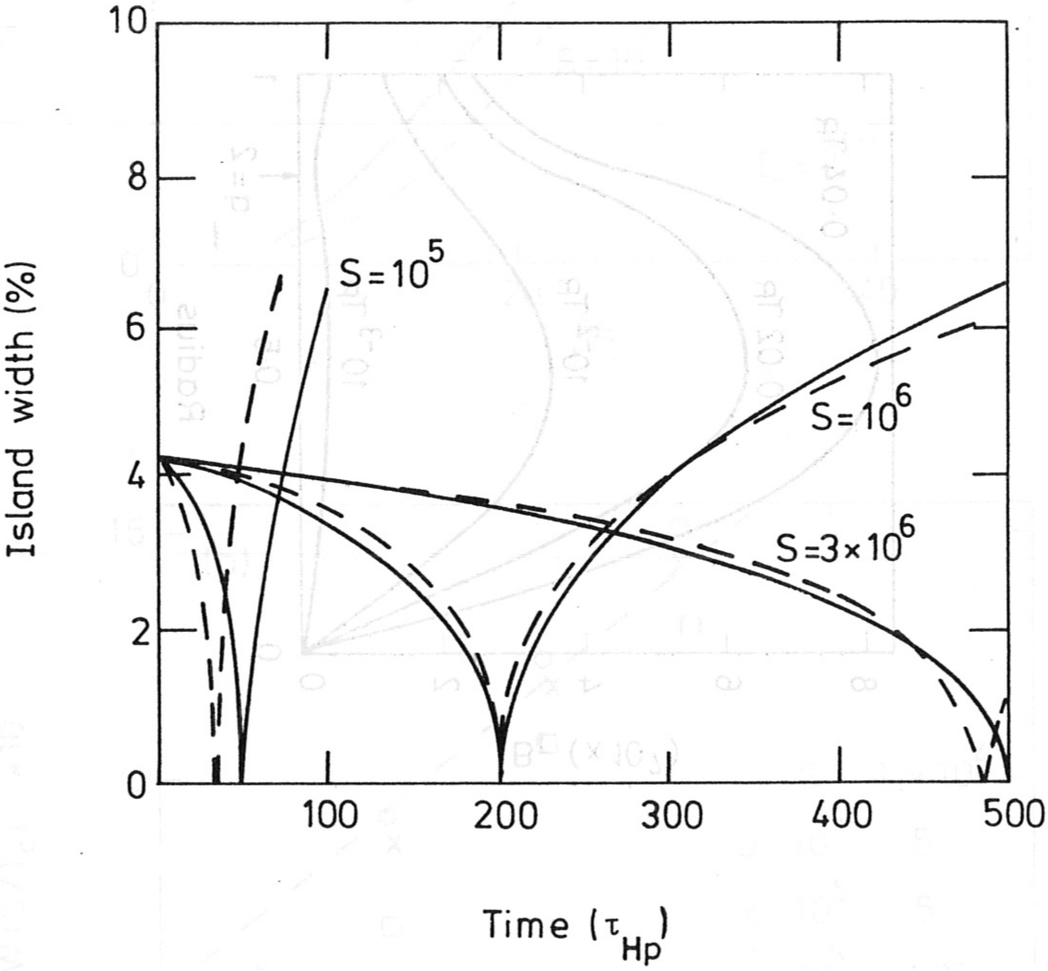

Island width (%)
Time (τ_{Hp})
S=10^5
S=10^6
S=3×10^6
0
2
4
6
8
10
100
200
300
400
500

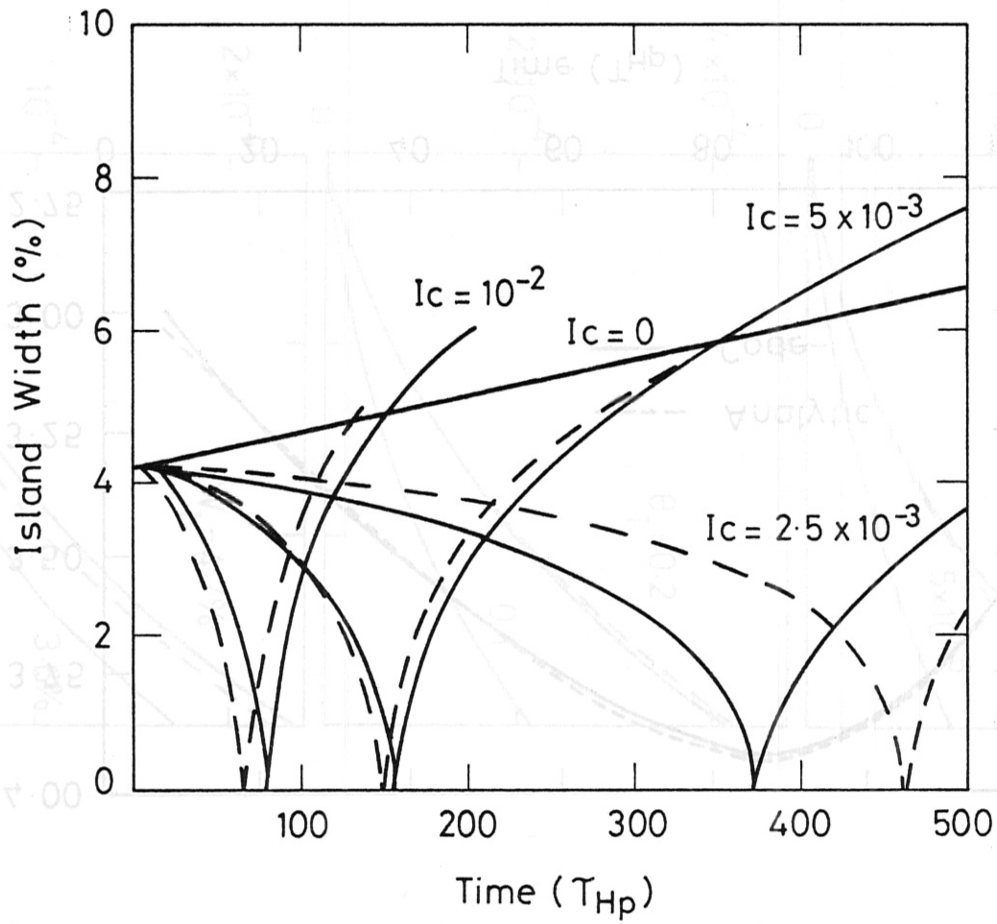

Island Width (%)
Time (T_{Hp})
Ic = 5 x 10^-3
Ic = 10^-2
Ic = 0
Ic = 2·5 x 10^-3

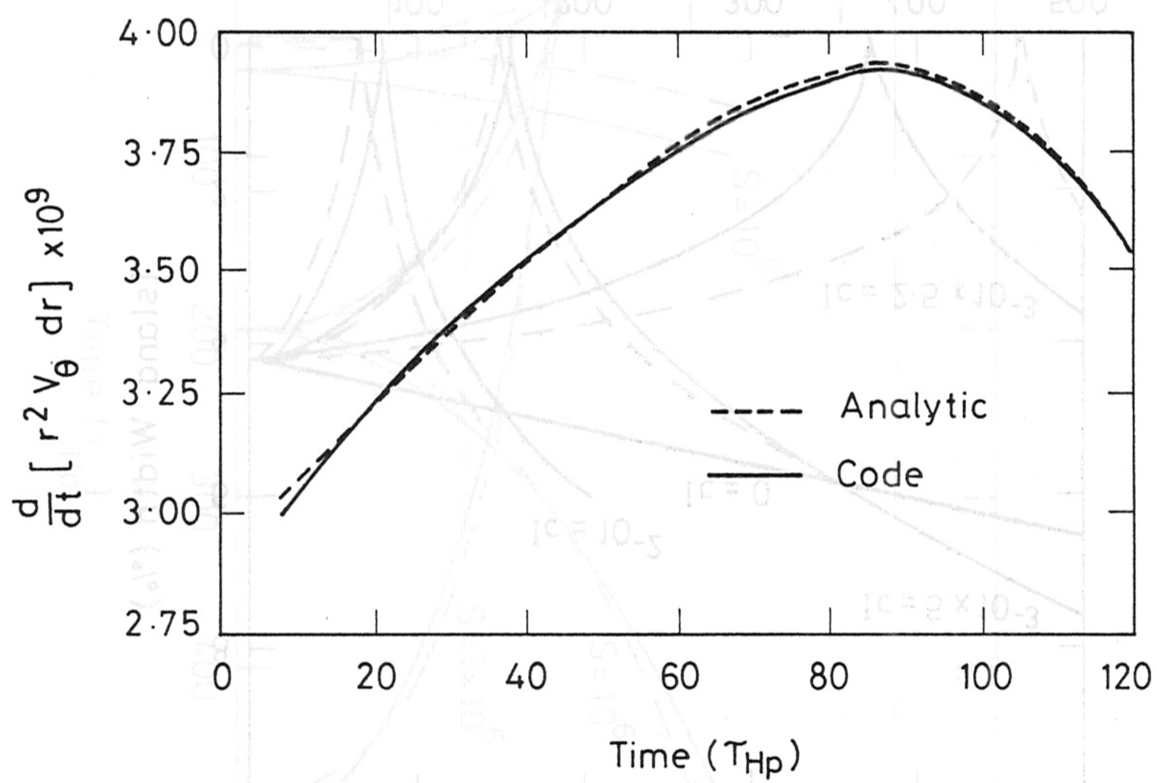
4·00
3·75
3·50
3·25
3·00
2·75
0
20
40
60
80
100
120
Analytic
Code
Time (τ_{Hp})
$\frac{d}{dt}[\int r^2 V_\theta \, dr] \times 10^9$

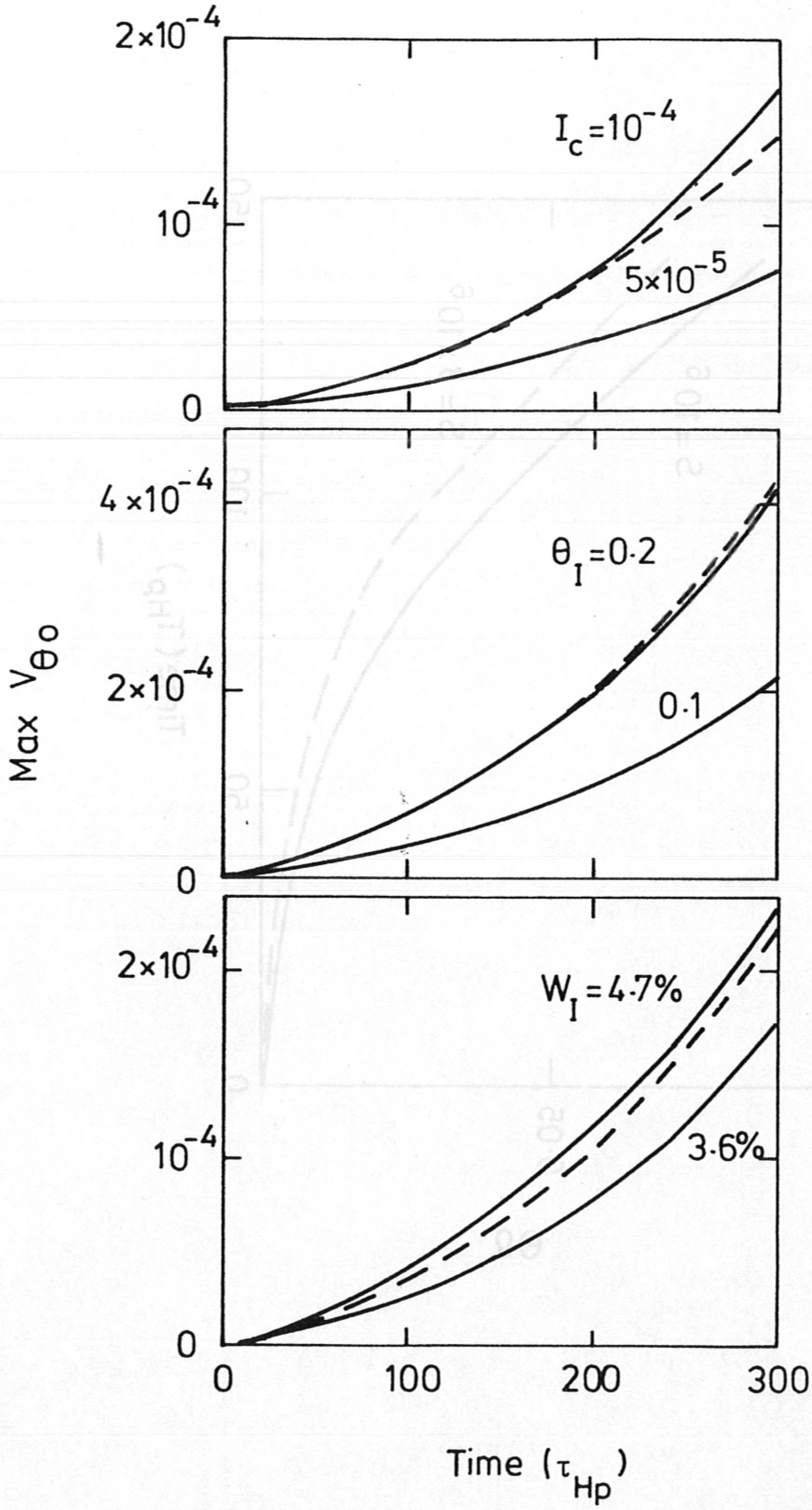

2×10⁻⁴
10⁻⁴
0
I_c = 10⁻⁴
5×10⁻⁵
4×10⁻⁴
2×10⁻⁴
0
θ_I = 0·2
0·1
2×10⁻⁴
10⁻⁴
0
W_I = 4·7%
3·6%
Max V_θo
0
100
200
300
Time (τ_Hp)

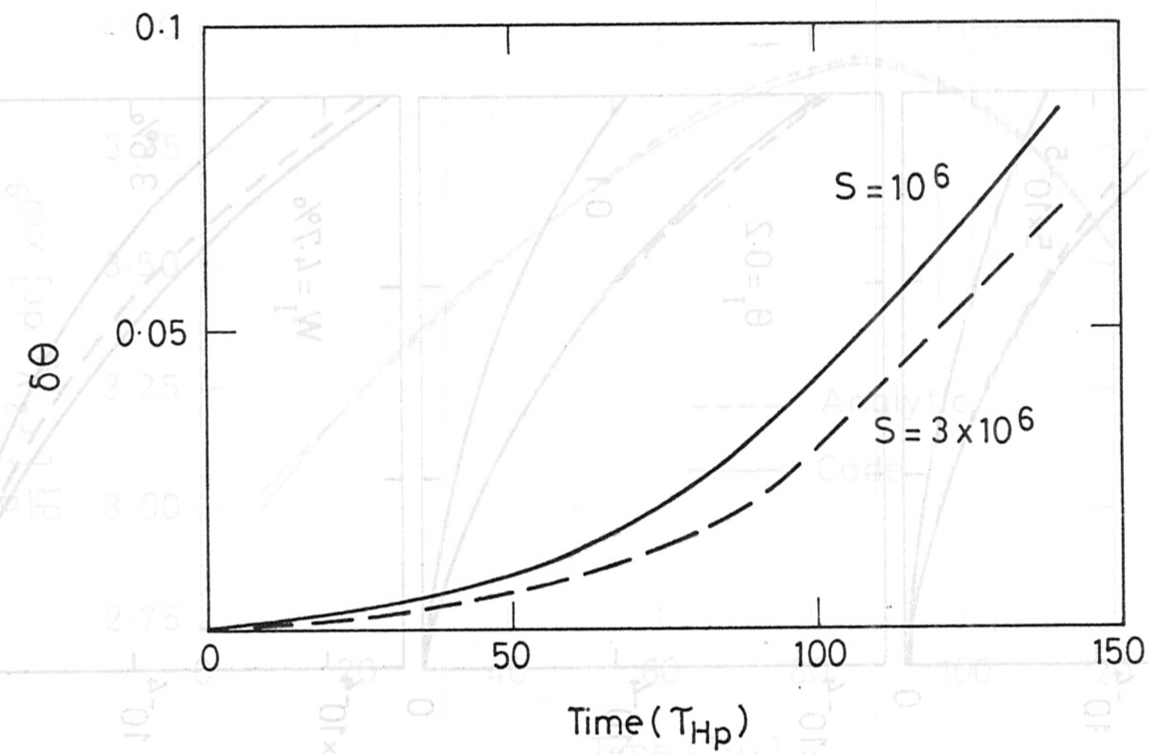

0·1
0·05
δΘ
0
50
100
150
Time (T_{Hp})
S = 10 6
S = 3 x 10 6